Particle Accelerators, 1996, Vol. 53, pp. 77–96
Reprints available directly from the publisher
Photocopying permitted by license only

INFLUENCE OF SURFACE ROUGHNESS AND PREPARATION, BULK PURITY AND HEAT TREATMENT ON ELECTRON FIELD EMISSION FROM Nb AND Nb_3Sn

N. PUPETER, A. GÖHL, T. HABERMANN, A. KIRSCHNER, E. MAHNER, G. MÜLLER and H. PIEL

Fachbereich Physik, Bergische Universität Wuppertal, Gaußstr. 20, D-42097 Wuppertal, Germany

(Received 7 February 1996; in final form 7 February 1996)

DC field emission studies on cm^2-sized Nb samples are presented in dependence on wet surface preparation, properties of bulk and surface, heat treatments and after coating with Nb_3Sn. A strong reduction of enhanced field emission (EFE) from Nb up to 200 MV/m was achieved by an improved chemical surface treatment. The density of emitters was 2–3 times higher on chemically polished Nb of low purity (RRR 30) than of high purity (RRR 250) material. Also the activation of emission from formerly inactive particles by heat treatments at 400°C in UHV depended strongly on the bulk purity. First studies on Nb_3Sn coatings on Nb, which would allow a reduction of the operational costs of accelerating structures, showed encouraging low emitter densities up to 70 MV/m. A statistical evaluation of the emission parameters of a large number of emitters resulted in a new correlation of the Fowler-Nordheim parameters β and S. The data could not be explained by pure geometrical field enhancement alone, but suggest a more complex process of enhanced field emission.

Keywords: Superconducting RF cavities, field emission

1 INTRODUCTION

The maximum attainable electrical accelerating field strengths in superconducting Nb cavities are limited either by enhanced electron field emission (EFE) or by thermal instabilities (quenches).[1] It is well known that EFE takes place locally at micron-sized particles or surface defects. However, the localisation and investigation of such emission sites is not possible in complex shaped cavities. Since no general difference between RF and DC field emission is expected,[2] a DC field emission scanning microscope was

built in Wuppertal.[3] By means of this apparatus, the density and properties of emitters on the damaged surface layer of unpolished Nb samples and on improved chemically polished Nb samples were measured. The influence of the Nb bulk purity on EFE after chemical polishing and after UHV heat treatments was investigated. In order to compare Nb with other promising materials for future superconducting accelerators, first studies on Nb_3Sn coated Nb samples were performed. Additionally, we aimed at a better understanding of the process of EFE and the still unknown physical meaning of the Fowler-Nordheim (FN) parameters β (geometrical field enhancement factor) and S (effective emitting area).

2 EXPERIMENTAL SET-UP AND PROCEDURE

The field emission scanning microscope (FESM) is integrated in a commercial UHV surface analysis system (Figure 1). A heating station in the preparation chamber allows heat treatments of samples up to 2000°C. The samples can be transferred to the FESM in the main chamber without breaking UHV.

By means of the FESM, field emission (FE) maps of cm^2-sized surfaces can be obtained. For that purpose, the sample is moved in a raster pattern below a tungsten anode tip at a constant gap, controlled by a long-range optical microscope. During this scan a high voltage is applied at the anode, and the small area below its tip is exposed to a high electrical field. If an emission site arrives at this field region current arises very quickly. In order to avoid the destruction of the emitter, the voltage is reduced by a fast regulator until a constant current (typ. 10 nA) is achieved. The plots of the voltage reduction versus sample position allow the simultaneous localisation of strong and weak emitters with coarse or fine resolution depending on the anode tip size. After a further localisation by a tungsten micro-tip anode with micron resolution, the onset field strength E_{on} and the local gap between the electrodes is determined very precisely for the single emission sites. The β and S values of each emitter are calculated from its IV characteristics. The morphology of an emitter can be depicted by means of an *in situ* scanning electron microscope (SEM), and its elemental composition can be detected by a hemispherical auger spectrometer (AES). At present, the analysis system is supplemented by a micro-focus ion sputter gun (spot size: 30 μm). A more detailed description of the system and the experimental procedure is given elsewhere.[3,4]

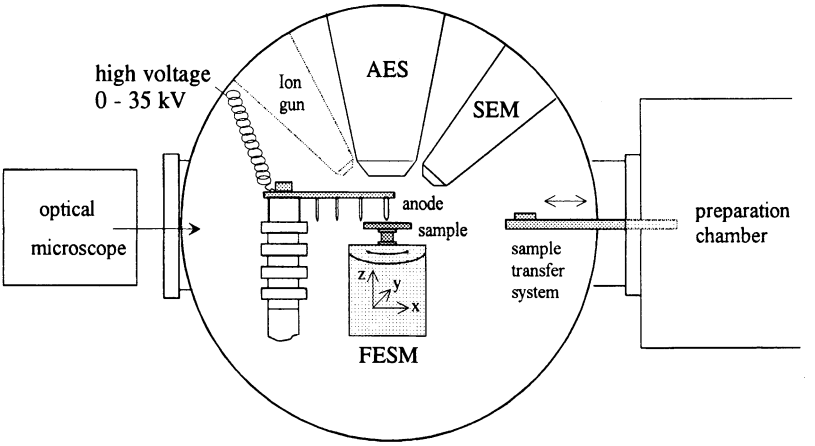

FIGURE 1 Schematic view of the apparatus for DC field emission studies. The sample is transferred from the preparation chamber into the center of the UHV chamber and analysed by the field emission scanning microscope (FESM), the scanning electron microscope (SEM) and the auger electron analyser (AES). The ion sputter gun is incorporated at present.

3 FIELD EMISSION MEASUREMENTS

In the following chapters the results of systematic FE studies on Nb samples are presented. Detailed studies were performed on EFE in dependence on surface roughness, chemical polishing, the purity of the bulk Nb and UHV heat treatments and after coating with Nb_3Sn.

3.1 Surface Roughness

During the production of accelerating cavities, a damage of the Nb surface cannot be avoided. Therefore, we have investigated the influence of the damage layer and surface roughness on EFE. In Figure 2 field emission maps at 100 MV/m and SEM images of the surfaces of 4 Nb samples with different amounts of surface removal by buffered chemical polishing (BCP) are shown. After a final ultra-pure water rinsing at DESY, emission appeared on these samples only from surface defects. Without chemical polishing, very strong emission was detected, often from sharp features at scratches or grooves (Figure 2a). The emission was drastically reduced after 4 μm surface

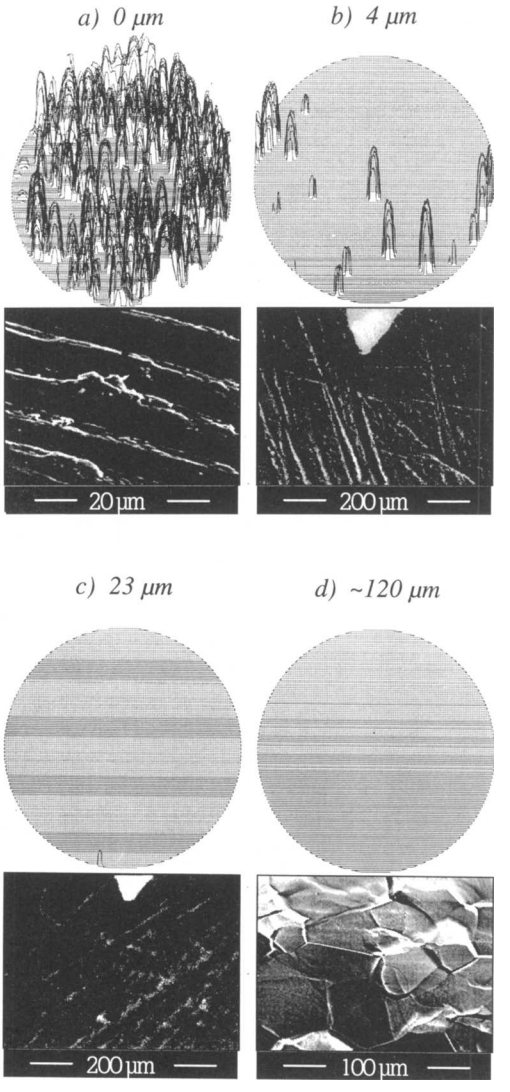

FIGURE 2 FE scans (E = 100 MV/m, area: $\oslash$ = 13, 5 mm, $I \leq 10$ nA) of Nb samples without BCP (a) and after 4 μm, 23 μm and ~120 μm surface removal (b-d, respectively). The SEM images show the typical surface structure of these specimens.

removal by BCP, although the roughness seemed macroscopically unchanged (Figure 2b). Already after a removal of 23 μm, the micro-roughness seemed to be smoothed and emission was suppressed up to 100 MV/m (Figure 2c). After a large amount (> 50 μm) of chemical polishing (Figure 2d), we never observed emission up to 200 MV/m caused by the roughness of the typical Nb grain structure. Despite of some foreign elements often found close to surface defects,[5] it is probable that the strong emission from rough surface defects is mainly caused by their geometrical field enhancement.

Further measurements showed no significant influence of the surface roughness on the removal of particulate contamination by ultra-pure water rinsing, but that will be subject of more comprehensive studies.

3.2 Improved Wet Surface Preparation

In order to create improved final preparation steps for the wet-chemical treatment of Nb cavities, we have investigated 8 Nb samples (RRR = 250), which were chemically polished in the usual way (120 μm by BCP 1:1:2). Additionally, 2 μm were removed in fresh acid. To avoid a hot reaction of a remaining acid film on air, we diluted the acid instantly with a large amount of pure water before taking the samples out of the acid container.

Six samples were rinsed in a large pool of pure water until the resistance of the water reached a value of 12 MΩcm. Then the surfaces were rinsed with a ultra-pure water jet (18 MΩcm), instantly followed by a removal of water drops by means of a class 10 N_2 jet. The FE measurements of these specimens showed a very strong reduction of EFE up to 200 MV/m.[5,6] In comparison to results of Ph. Niedermann (1986),[7] we achieved 100 times lower emitter densities at 50 MV/m.

Three of the six samples were anodised to a 110 nm oxide layer before the ultra-pure water rinsing. Surprisingly, no influence of the oxide layer on the density and properties of emitters was detected up to 200 MV/m.

Two other samples were chemically polished in the same way as described above but rinsed only with water of lower purity and resistance (0.3 MΩcm). These samples showed a 7 times higher emitter density at 100 MV/m, and larger particles were identified as emission sites on average.

Typical examples of emitting particles after rinsing with water of different purity are shown in Figure 3. In Figure 4 the size of the localised emitters is plotted versus their onset field strength E_{on}. Considering that only a small percentage of the particles found on the surface emits below 200 MV/m,

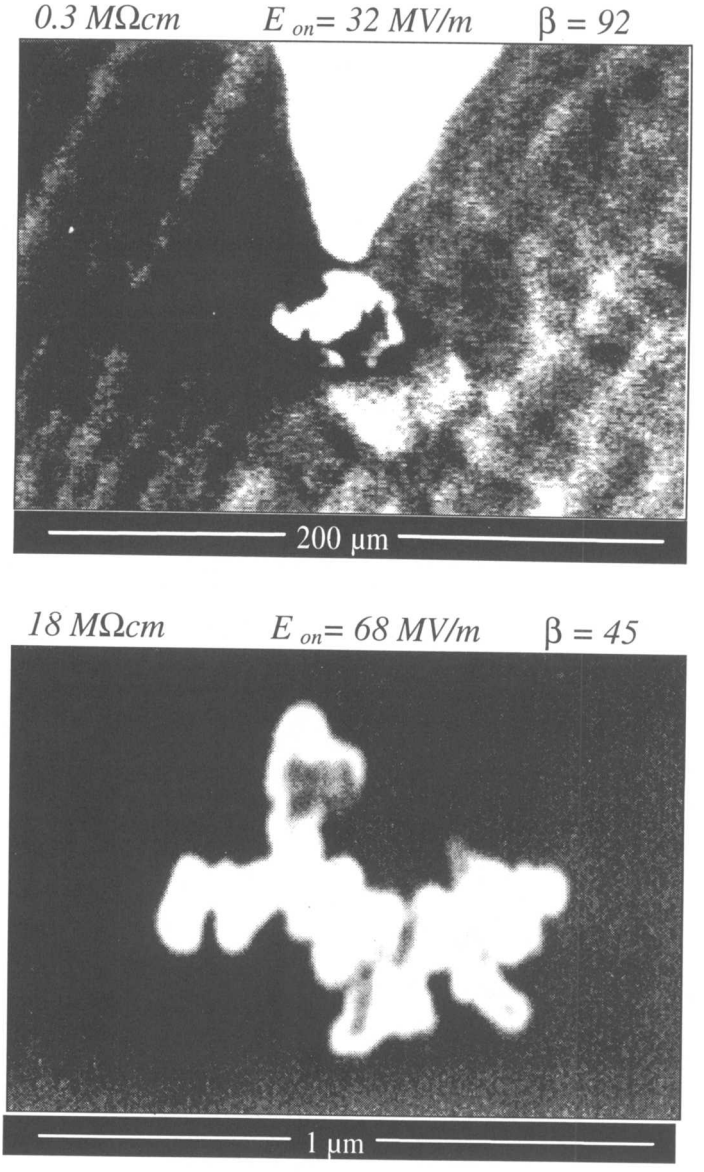

FIGURE 3 SEM micrographs of typical emitting particles, localised after final rinsing with water of low purity (above) and high purity (below). Please take note of the different scales.

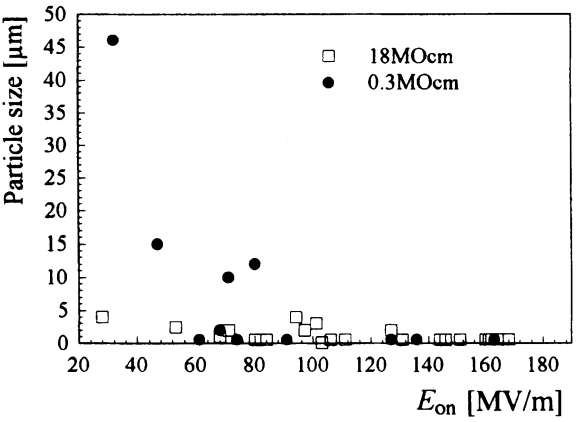

FIGURE 4 The size of emitting particles versus their onset field strengths for $I = 0.5$ nA for different qualities of the final water rinsing.

no correlation between particle size and E_{on} is visible. But it is obvious that ultra-pure water rinsing (18 MΩcm) allows a strong reduction of larger particles (> 5 μm), which tend to emit already at low field strength. Besides the water purity, the drying procedure of wet surfaces is important, too. Replacing the instant water removal by means of a nitrogen jet with a slow drying of Nb samples in the class 10 clean room lead to EFE from particulate contamination in dried drops even after rinsing with 18 MΩcm. Further FE studies are required to check how far the described improvements can be applied to multicell accelerating structures.

3.3 Purity of Niobium (RRR)

The influence of the purity of the bulk Nb on the EFE behaviour was not investigated until now. Therefore, we investigated 3 pairs of Nb samples with different degrees of purity, as given by their residual resistance ratio (RRR). About 170 μm were removed by BCP (1:1:1) at CEBAF from all 6 samples. After a high-pressure (~80 bar) ultra-pure (18 MΩcm) water rinsing, a final rinsing with electronic grade-methanol was performed.

In Figure 5 the density of emission sites with $I \geq 10$ nA found at different electrical field strengths at these samples with RRR values of 30, 250 and

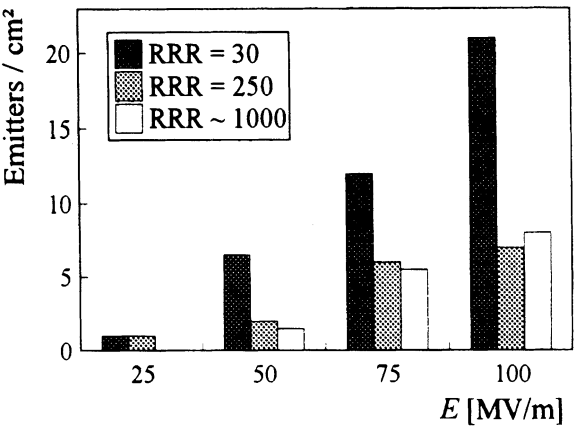

FIGURE 5 Density of emitting sites versus electrical field strength on chemically polished Nb samples of 3 different purity grades (RRR).

1000 is shown. On these samples all localised sites were identified as particle emitters. While the Nb samples with RRR = 250 and 1000 yield similar emitter densities, the RRR 30 samples showed a 2–3 times larger density of emitting particles between 50 MV/m and 100 MV/m.

This strong influence is not easy to understand, because EFE is supposed to be a pure surface phenomenon. We assume a large percentage of the contamination in Nb of RRR = 30 as clusters of metallic inclusions (e.g. Ta) or oxides. Uncovered by the chemical polishing, some of such inclusions might dissolve only slowly into the BCP or survive in the acid. At the end of the polishing, such clusters could stick on the Nb surface. In this case, the remaining density of emitting particles would be in inverse proportion to the original bulk purity. Moreover, this explanation underlines the importance of a final surface removal of only some microns in fresh acid in good agreement with the results of the previous sub-section 3.2.

3.4 UHV Heat Treatments

In previous experiments we measured a strong influence of UHV heat treatments on the FE behaviour of Nb surfaces.[3,4,6,8] All types of emitting

sites can be deactivated by heating at 1400°C for 30 min. In contrast, heat treatments between 200°C and 800°C result in a strong activation of emission from formerly inactive particles on both chemically polished surfaces and on 1400°C heat-treated surfaces. This activation could be critical for the annealing of cavities, because they stay several hours during the cool down between 800°C and 200°C. Fortunately, we observed that a new activation at lower temperatures can be strongly reduced by a longer heating (> 3 h) at 1400°C.

Figure 6 shows 2 particles, which were activated to emission by 400°C annealing. Particularly the right one of ~200 nm size proves that very small particles can strongly emit. The activation could be associated with surface diffusion or segregation of interstitial atoms from or into the bulk Nb. Therefore, we started to look for a correlation between the density of activated sites and the purity of the bulk material. All 6 Nb samples, described in sub-section 3.3 with RRR = 30, 250 and 1000, were heated for 60 min at 400°C. The densities only of the new activated emitters is plotted versus the electrical field strength in Figure 7. The density of activated sites is about 7 times larger for the lowest than for the highest RRR material. In contrast to the results on non-heated samples, there is also a significant difference between the RRR = 250 and 1000 samples. These results suggest that the bulk purity influences the activation process more than the number of particles itself, which might be larger for lower purity grade material. A transition of phase and/or a change of conductivity of Nb oxides between 400°C and 1400°C would drastically influence the properties of the interface between the particle and the substrate.

In order to identify a change of the elemental surface composition after heating, we have taken integral Auger spectra of the samples of different bulk purity. As expected for surfaces with oxides and adsorbates, there is no significant difference in elemental composition before the heating. The main peaks are from Nb oxides and adsorbed gases (C, O). After heating at 400°C for 60 min, the oxygen/Nb ratio is strongly reduced.

The carbon/Nb ratio shows a smaller reduction and carbide sub-peaks occurred. Enhanced carbon concentration was detected in previous experiments[7] in correlation with an activation of emission sites on Nb by heating between 200°C and 800°C. Traces of sulphur were detected as the only other foreign element, astonishingly most pronounced on the purest niobium. Considering the similarity of the Auger spectra for samples of different purity grade, however, there is no significant hint for surface diffusion or segregation of

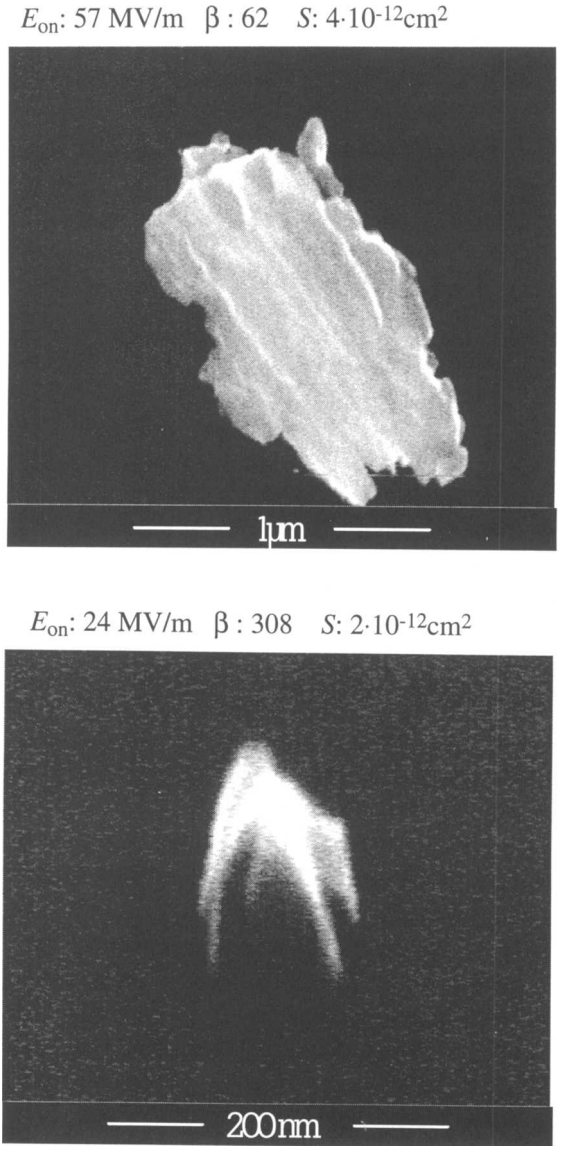

FIGURE 6 SEM micrographs of particles, which were activated to EFE by heat treatments at 400°C for 60 min in UHV. The emission parameters E_{on}, β and S are listed above the images.

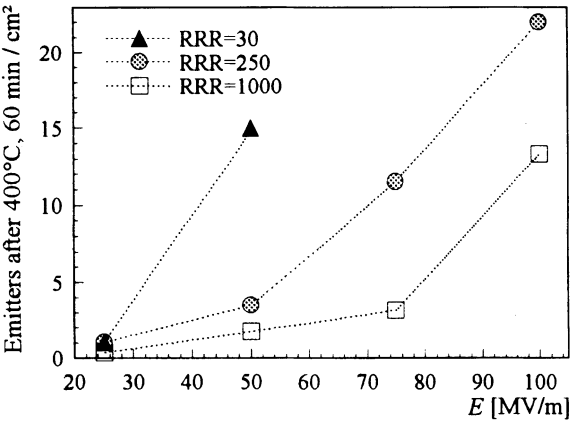

FIGURE 7 Density of activated emitters after 400°C, 60 min versus electrical field strength for Nb samples of different purity.

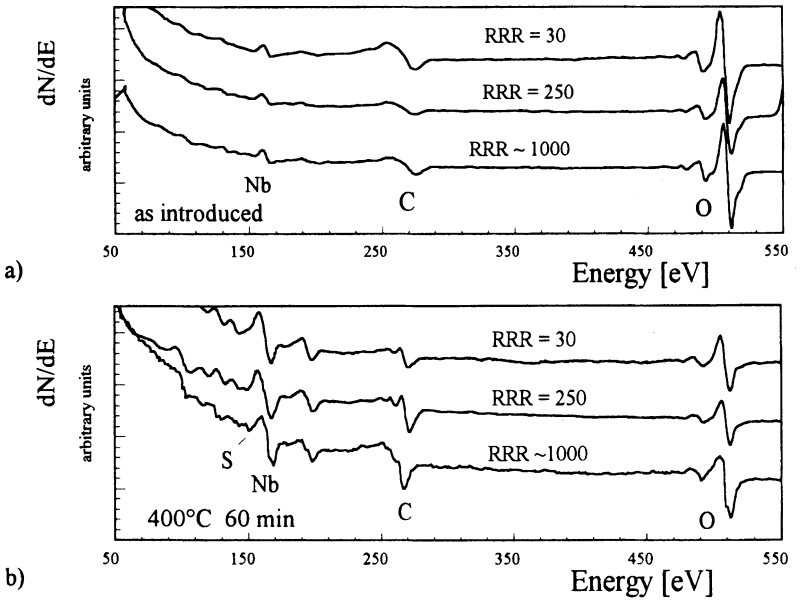

FIGURE 8 Auger spectra taken from 1 mm squares on non-heated (a) and 400°C, 60 min heat treated (b) Nb samples of different RRR values.

interstitial atoms except C and O, that could explain the observed activation phenomenon. Therefore, spatially resolved micro-Auger analysis and ion bombardment of the emitter regions have to be performed to clarify the role of impurities for EFE.

3.5 Nb_3Sn

The production and operational costs of superconducting accelerators depend strongly on the cryogenic temperature. Whereas Nb cavities in the average need an operation temperature below 2 K, Nb structures coated with Nb_3Sn would allow operation at 4.2 K. First experiments of 1.5 GHz Nb_3Sn-coated high purity Nb structures showed very promising results.[9] Therefore, the FE behaviour of Nb_3Sn coatings becomes important for their technical suitability. Three Nb samples (RRR = 250, $\oslash$ = 16 mm) were chemically polished ~185 μm in BCP 1:1:1 in Wuppertal. Finally, 2.5 μm were removed in fresh acid. One sample was anodised at 50 V, i. e. to 70 nm $\pm$ 10 nm. After nucleation with $SnCl_2$ (0.5 h, 460°C–595°C), a Sn vapour deposition (3 h, 1150°C) followed. Finally a tempering at 1150°C for 30 min was performed. In this way a 1.5 ± 0.1 μm thick Nb_3Sn coating was created on the 3 samples. Finally, all samples were ultra-pure (18 MΩcm) water rinsed and showered with a class 10 N_2 jet in the clean room facility at DESY.

The FE measurements resulted in similar densities and properties of emitters for all 3 samples, i.e. no correlation to the anodisation or the additional tempering. The average emitter density on Nb_3Sn was higher than that of the best Nb samples (3b) but astonishingly low at the first attempts. The emitter analysis showed promising results. All analysed sites were identified as contamination of foreign elements (Fe, Cr, Ni, Al). Typical examples of the analysed sites are shown in Figure 9. Because the Nb_3Sn morphology dominates around those contamination, it seems that the contamination must have been on the Nb substrate before the Sn deposition. No intrinsic emission from the pure Nb_3Sn grain structure was detected up to 200 MV/m. Therefore, an improved chemical treatment and a more careful handling of the Nb before the Sn deposition should allow the same strong reduction of the emitter density on Nb_3Sn as on Nb (3b).

4 STATISTICS

A comparison of emitter densities at relevant field strengths is necessary for the assessment of the quality of different preparation methods. In Figure 10

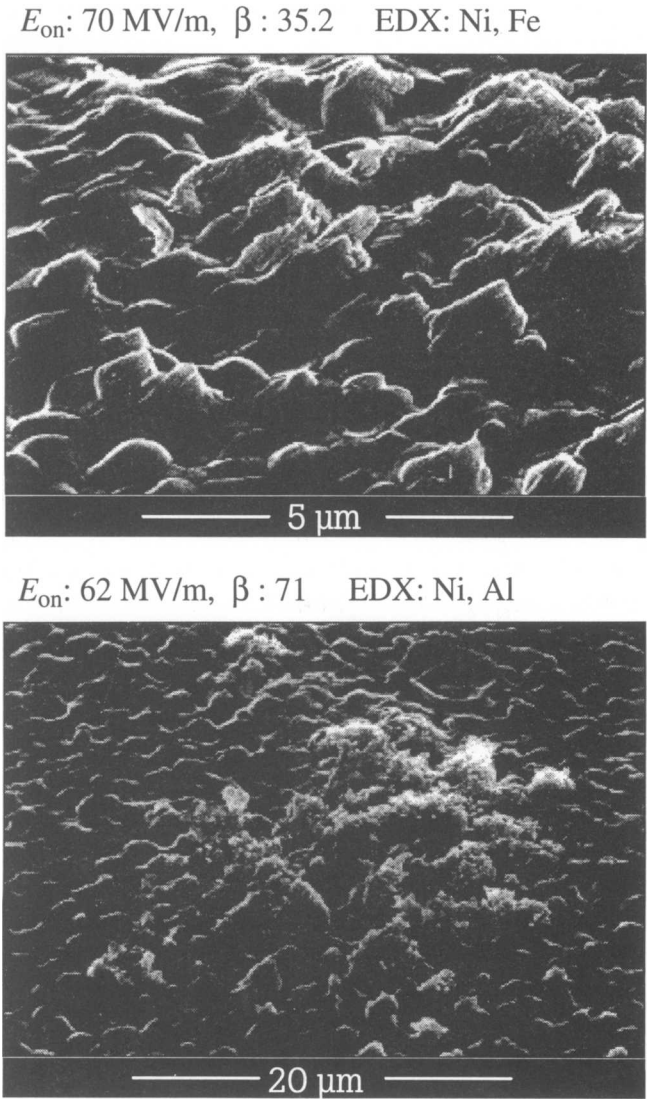

FIGURE 9 Typical SEM images of Nb_3Sn coatings with emitting contamination. The top emission site is part of a ~1 mm long and ~50 wide trace of Ni contamination. E_{on}, β and the elemental composition (except Nb and Sn) are given above the images.

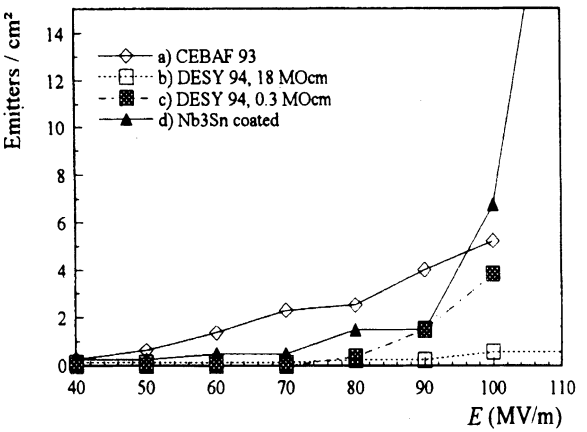

FIGURE 10 Density of emission sites versus electrical field strength for different surface preparation: (a) BCP 1:1:1 at CEBAF, high-pressure ultra-pure water rinsing, methanol rinsing.[8,10] (b) Improved BCP 1:1:2 (3b) at DESY, followed by a ultra-pure water rinsing (18 MΩcm). (c) as (b) but water resistance only 0.3 MΩcm. (d) Nb samples coated with 1.5 μm Nb_3Sn.

the emitter densities on Nb samples after 3 different wet-chemical preparations and after coating with Nb_3Sn are presented. The Nb_3Sn samples (d) showed very good results up to 90 MV/m. Above this field level the emitter density rises exponentially. That could limit the suitability of Nb_3Sn in accelerating structures to moderate gradients, but more comprehensive studies are necessary. Compared to previous results after chemical polishing at CEBAF (a),[8,10] 5 to 10 times smaller emitter densities were achieved between 50–100 MV/m by the improved chemical preparation at DESY (b). The comparison of the results after a final water rinsing with a resistance of 18 MΩcm (b) and 0.3 MΩcm (c) shows the importance of the water purity on the reduction of EFE.

An extraordinary large number of individual emission sites was analysed within the scope of our FE studies.[4] The morphology of 291 emitters was *in situ* investigated by means of our SEM. 44% of the sites were identified as micron or submicron-sized particles. The structure of 33% of the emitters was too small for a identification within the resolution (500 nm) of our SEM. Surface defects were in 19% of the analysed sites the source of emission.

The frequency of the different emitter types depended on the preparation technique. Generally, it should be easier to avoid emission from surface defects, than from submicron-sized particles. Never intrinsic emission from the polycrystalline Nb or Nb_3Sn grain structure was detected.

The evaluation of the measured IV characteristics proves that 59% of the emitters showed stable emission, which was fitted very well by the modified FN law:

$$I(E) = \frac{AS\beta^2 E^2}{\phi} \times \exp\left(\frac{-B\phi^{3/2}}{\beta E}\right) \tag{1}$$

that describes the emission current I [nA] in dependence on the electrical field E [MV/m]. β is the geometrical field enhancement factor, S [cm^2] the effective emitting area and ϕ [eV] the workfunction. $A = 1.54 \cdot 10^{11}$ and $B = 6.83 \cdot 10^3$ are constants. Current instabilities at 34% of the sites resulted in jumps in the FN plots, which often changed not the β value but the S value for some orders of magnitude. Only 7% of the IV characteristics could not be fitted by the FN law. E_{on}, β and S of 300 different emission sites were determined and classified in dependence on sample preparation.

Figure 11 shows the distribution of E_{on} values versus the corresponding β values. A strong correlation was observed between E_{on} and β:

$$E_{on} \sim \beta^{-0.7} \tag{2}$$

That does not result inevitably from the FN law because of the $I(S)$ dependence. Additionally, for a constant S value a correlation of $E_{on} \sim \beta^{-1}$ would be expected. No statistical dependence of E_{on} on S was detected.

The physical meaning of the FN parameter S is often discussed controversially, because the very sharp microprotrusions, which are necessary to explain EFE purely by geometrical field enhancement,[11] could not be found on natural Nb surfaces even in high resolution SEM's. Most emission sites were identified as particles, so that meaningful limits for the emitting area can be given by 10^{-6} cm^2 and 10^{-12} cm^2, which correspond to particles between 10 μm and 10 nm size. In Figure 12 the distribution of S values of 302 different emitters is plotted versus the corresponding β values. β and S are calculated with the assumption of a work function of $\phi = 4$ eV and without image force correction.

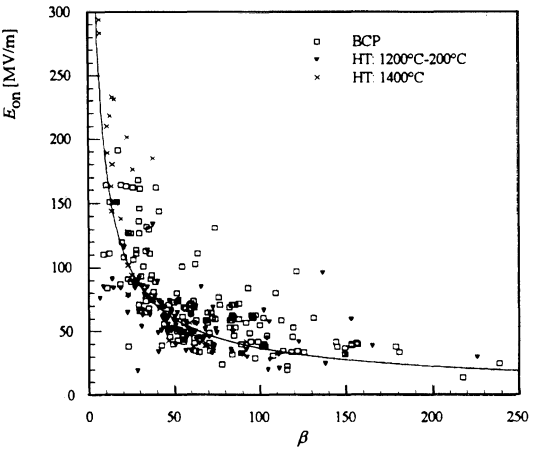

FIGURE 11 Onset field strength E_{on} for $I = 0.5$ nA plotted versus the corresponding β values.[4] The emitters are classified in relation to the sample preparation as chemical polishing (BCP), heat treatments (HT) between 200°C and 1200°C, and HT at 1400°C.

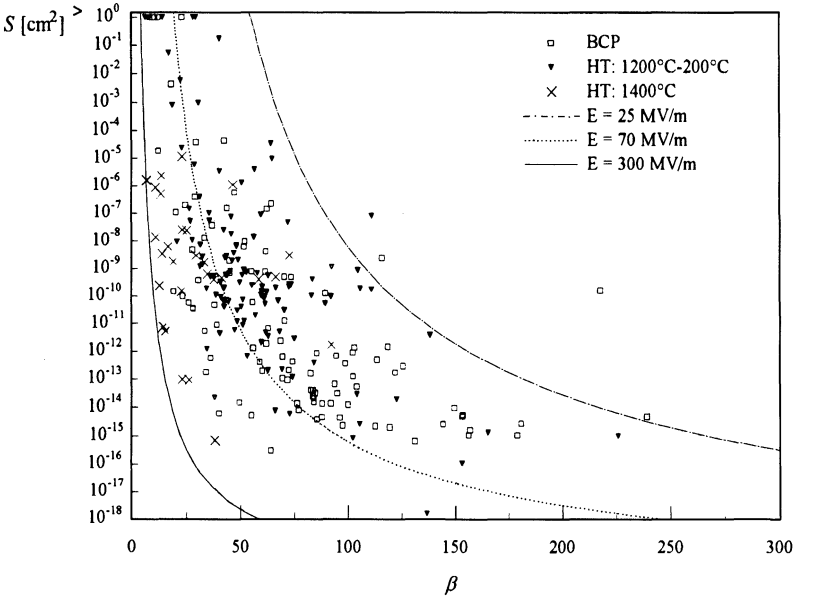

FIGURE 12 Fowler-Nordheim fit parameter S plotted logarithmically versus the corresponding β value for the same classification as in Figure 11.[4] In the graph 3 theoretical lines of constant E_{on} (β, S) for $I = 0.5$ nA are plotted.

Astonishingly, the S values show a large spread of more than 18 orders of magnitude. About 50% of the S values are outside of the above discussed realistic limits of 10^{-6} cm^2 and 10^{-12} cm^2. Estimations from the FN law with a given slope $(\ln(I/E^2))/(1/E)$ of the IV curve prove that this spread can not be explained by the neglect of image force correction or by deviations in the unknown local work function. A variation of ϕ between 0.5 eV and 10 eV would result in a variation of the S values of only 2 orders of magnitude. If image force correction would be taken into account, all S values would be reduced about 2 orders of magnitude. Since β and S are independent parameters in the modified FN law, S should vary in physical meaningful limits, but should not be correlated to β. However, Figure 12 reveals a correlation between both parameters. Large β values are correlated with small S values and vice versa.

Because this correlation is a new result, all systematic errors and experimental influences have to be discussed. In the modified FN law the onset field strength E_{on} is a function of β and S. Therefore, 3 theoretical lines for constant E_{on} are plotted in Figure 12 to show which combinations of β and S result in strong or weak emission. Until now, no measurements above 420 MV/m were performed in the FESM. This means that we did not detect very weak emitters with low β *and* low S values, i.e. in the lower left corner of Figure 12. In contrast, nearly all samples were measured up to 100 MV/m, so that all strong emission sites with high β *and* high S values above the line of $E_{on} = 70$ MV/m should show up if present. Nevertheless, no sites with high β *and* high S values were measured. Moreover, the correlation is supported by the large variation of S values between strong and weak sites. Often unrealistic high S values ($S \gg 10^{-6}$ cm^2) were measured at weak emission sites with low β values, and emitters with high β values show often extreme small S values ($< 10^{-15}$ cm^2). Because the emission strength and E_{on} are correlated to β but not to S, we assume β but not S as intrinsic parameter of the emission process. This agrees well with the observation that in case of unstable IV characteristics the S value changes more often than β.

Another puzzling factor is the size of emitting particles and its influence on the emission strength. As size A of an emitter, we determined the average diameter of the particle in the SEM. This evaluation resulted in no correlation between particle size and E_{on}, S and β. This result is not very astonishing, because EFE probably arises only from a small part of the particle, while its size only affects the field distribution. In order to test theoretical models which

try to explain EFE purely by geometrical field enhancement, the correlation of S and A has to be discussed. For simple metallic microprotrusions of height h and radius r on top of a particle of the size A, β and S should be related to A as follows:

$$A \geq h \approx \beta \cdot r \sim \beta \cdot \sqrt{S} \tag{3}$$

In the later developed model of superimposed microprotrusions[11] this requirement is even enforced with:

$$A \gg \beta \cdot \sqrt{S} \tag{4}$$

In Figure 13 ($\beta\sqrt{S}$) is plotted versus the observed particle size A. In case of purely geometrically enhanced emission all data should be on or below the marked line of $A = \beta\sqrt{S}$. Obviously, however, most emitters in Figure 12 are too small to accommodate ultra-sharp micro protrusions which could explain the detected high β and S values. This means that EFE cannot be explained by simple geometrical field enhancement alone. A new, more complex model has to be developed, which takes the influence of the interface between particle and substrate as well as of a locally reduced work function into account.

5 SUMMARY

Damage of the Nb sheet material during the normal production process causes very strong EFE from scratches or other surface defects. Already a removal of about 20 μm by BCP can suppress this emission. Intrinsic emission from the pure, typical grain structure of Nb was never detected after a large amount of chemical polishing (> 50 μm). An improved wet-chemical preparation was developed, which strongly reduced EFE on Nb up to 200 MV/m. No influence of additional oxide layers on the FE behaviour of Nb was observed. Nb of low purity (RRR = 30) showed after BCP 2–3 times higher emission densities than material of RRR = 250 or 1000. A long (> 3 h) heating at 1400°C could strongly reduce the activation of EFE from particles between 200°C and 800°C. The density of activated particles was about 7 times larger for Nb of RRR = 30 compared to Nb with RRR~1000. First experiments on Nb_3Sn-coated Nb samples showed low emitter densities up to 70 MV/m. All analysed emitters were identified as foreign element contamination, and no intrinsic emission from the rough, pure Nb_3Sn grain

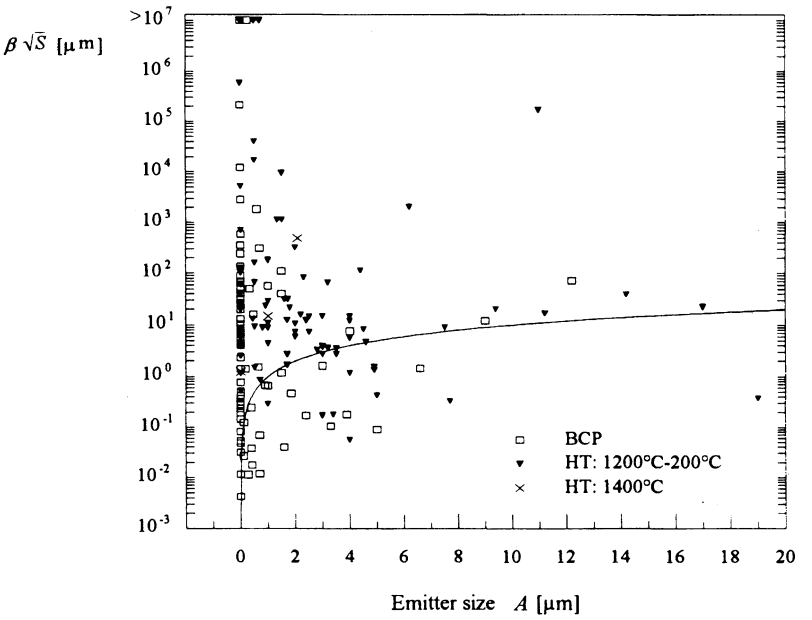

FIGURE 13 Theoretically calculated emission area ($\beta\sqrt{S}$) versus observed emitter size A for the same classification as in Figure 11.[4] The line corresponds to $\beta\sqrt{S} = A$.

structure was measured up to 200 MV/m. 44% of all investigated emission sites on Nb were identified as micron-sized particles sticking on the surface. 59% of the emitters were stable and could be fitted well by the modified FN law. A new correlation was found between the theoretically independent FN parameters β and S. High β values are correlated to small S values and vice versa, and β seems to be the intrinsic parameter of the emission process. Statistical evaluation proved that the process of EFE can not be described by pure geometrical field enhancement. A new and more complex model has to be developed, which takes a locally reduced work function and the influence of the interface between the particle and the substrate into account.

Acknowledgements

These studies were generously supported by DESY. The authors wish to thank A. Matheisen for his assistance during sample preparation in the TTF

clean room facility. Furthermore we wish to thank P. Kneisel for the fruitful co-operation and the comprehensive number of samples which he prepared at CEBAF.

References

[1] *Proc. of the 6th Workshop on RF Superconductivity*, editor R.M. Sundelin, CEBAF, Newport News, (1993).
[2] Noer, R.J. (1982). *Appl. Phys.*, **A28**, 1.
[3] Mahner, E., Minatti, N., Piel, H. and Pupeter, N. (1993). *Appl. Surf. Sci.*, **67**, 23.
[4] Mahner, E. (1995). *Ph.D. thesis*, No **WUB-DIS 95-7**.
[5] Mahner, E., Müller, G., Piel, H. and Pupeter, N. (1995). *J. Vac. Sci. Technol.*, **B 13(2)**, 607.
[6] Pupeter, N., Mahner, E., Matheisen, A., Müller, G., Piel, H. and Proch, D. (1994). *Proc. of the 4th Eur. Particle Accelerator Conf.*, **Vol. 3**, edited by Suller, V. and Ch. Petit-Jean-Genaz, London, 2066.
[7] Niedermann, Ph., Sankarramann, N., Noer, R.J. and Fischer, Ø. (1986). *J. Appl. Phys.*, **59(3)**, 892.
[8] Mahner, E. (1994). *Particle Accelerators*, **46**, 67.
[9] Röth, R., Kneisel, P. and Müller, G., *Proc. of the 7th Workshop on RF Superconductivity 1995*, Paris, to be published.
[10] Mahner, E., Kneisel, P., Pupeter, N. and Müller, G. (1993). *Proc. of the 6th Workshop on RF Superconductivity*, editor R.M. Sundelin, CEBAF, Newport News, 1085.
[11] Jimenez, M., Noer, R.J., Jouve, G., Jodet, J. and Bonin, B. (1994). *J. Phys. D: Appl. Phys.*, **27**, 1038.